



# Utilizing Flood Inundation Observations to Obtain Floodplain Topography in Data-Scarce Regions

Apoorva Shastry<sup>1,2\*</sup> and Michael Durand<sup>1,2</sup>

<sup>1</sup> School of Earth Sciences, The Ohio State University, Columbus, OH, United States, <sup>2</sup> Byrd Polar and Climate Research Center, The Ohio State University, Columbus, OH, United States

## OPEN ACCESS

### Edited by:

Paul Bates,  
University of Bristol, United Kingdom

### Reviewed by:

Andrew Mark Ireson,  
University of Saskatchewan, Canada  
Juan Pablo Rodríguez Sánchez,  
University of Los Andes, Colombia

### \*Correspondence:

Apoorva Shastry  
shastry.7@osu.edu

### Specialty section:

This article was submitted to  
Hydrosphere,  
a section of the journal  
Frontiers in Earth Science

**Received:** 06 October 2018

**Accepted:** 17 December 2018

**Published:** 11 January 2019

### Citation:

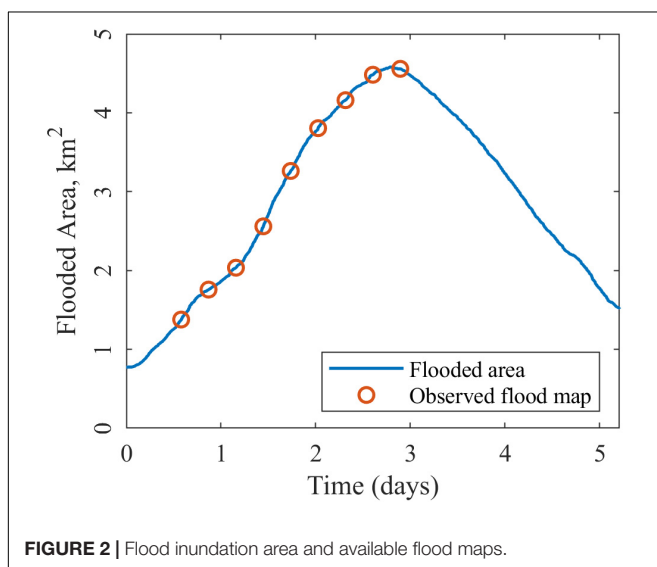
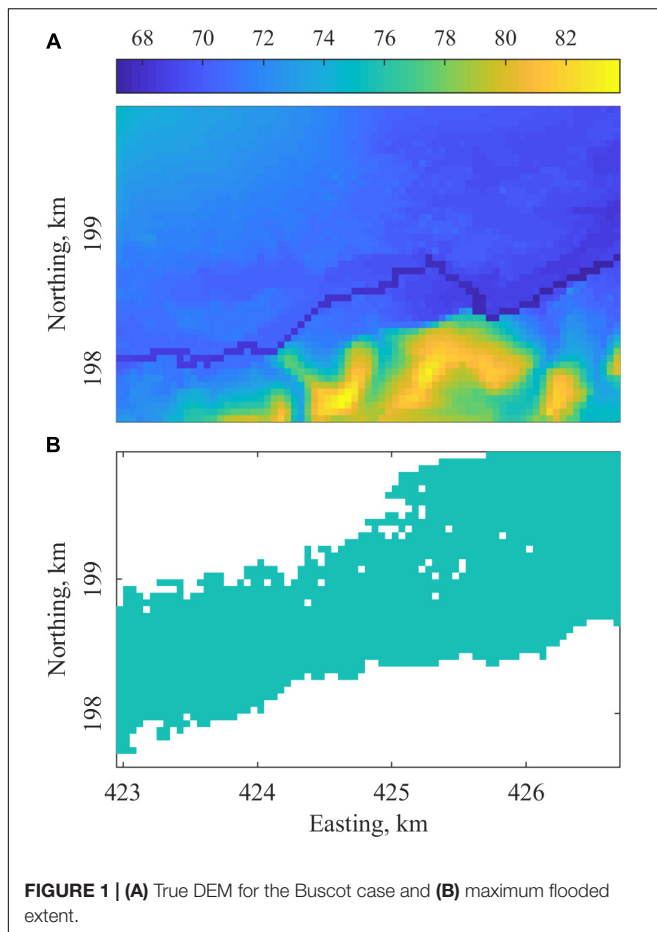
Shastry A and Durand M (2019)  
Utilizing Flood Inundation  
Observations to Obtain Floodplain  
Topography in Data-Scarce Regions.  
*Front. Earth Sci.* 6:243.  
doi: 10.3389/feart.2018.00243

Flood models predict inundation extents, and can be an important source of information for flood risk studies. Accurate flood models require high resolution and high accuracy digital elevation models (DEM); current global DEMs do not capture the topographic details in floodplains, and this often leads to inaccurate prediction of flood extents by flood models. Flood extents obtained from remotely sensed data provide indirect information about topography. Here, we attempt to use this information along with model predictions to produce better floodplain topography. The algorithm we describe is a two-step process: first, we reduce the noise along the observed flood boundaries for all particles. Then, the model predictions from these modified DEMs are assimilated with observations using a particle batch smoother. We implemented the algorithm for a synthetic test case. For the nominal case, we observed a significant improvement in accuracy in terms of RMSE (35% reduction), bias (20%), and standard deviation (40%). We conducted sensitivity analysis by using priors of varying bias (0.5, 1, and 2 m) and standard deviation (1, 2, and 4 m). The bias reduced to ~0.5 m or below in all the cases: the reduction in bias varied from 11 to 76%. The standard deviation of errors in the final estimate was almost half of the prior: the reduction varied from 40 to 49%. The reduction in RMSE ranged between 35 and 67%. For the case with 2 m bias and 4 m standard deviation (SRTM-like error levels), bias went down to 0.48 m (76% reduction), and standard deviation reduced to 2.24 m (44% reduction). Flood inundation maps produced from the final estimate DEMs also improved on its prior. For the 2 m bias cases, true positive rate (TPR) for peak inundation went from ~30% to more than 57% in all three cases. The algorithm produces promising results, and this type of analysis can be performed in data-poor floodplains where high resolution DEMs do not exist.

**Keywords:** digital elevation model, flood modeling, data assimilation, remote sensing, floodplains

## INTRODUCTION

Prediction of inundation extents from flood models is an indispensable source of information for assessing flood risk in the context of hazard studies, but inundation prediction accuracy is often limited by the quality of topographic data available globally. Topographic data, generally in the form of digital elevation models (DEMs), are the primary input data for flood inundation

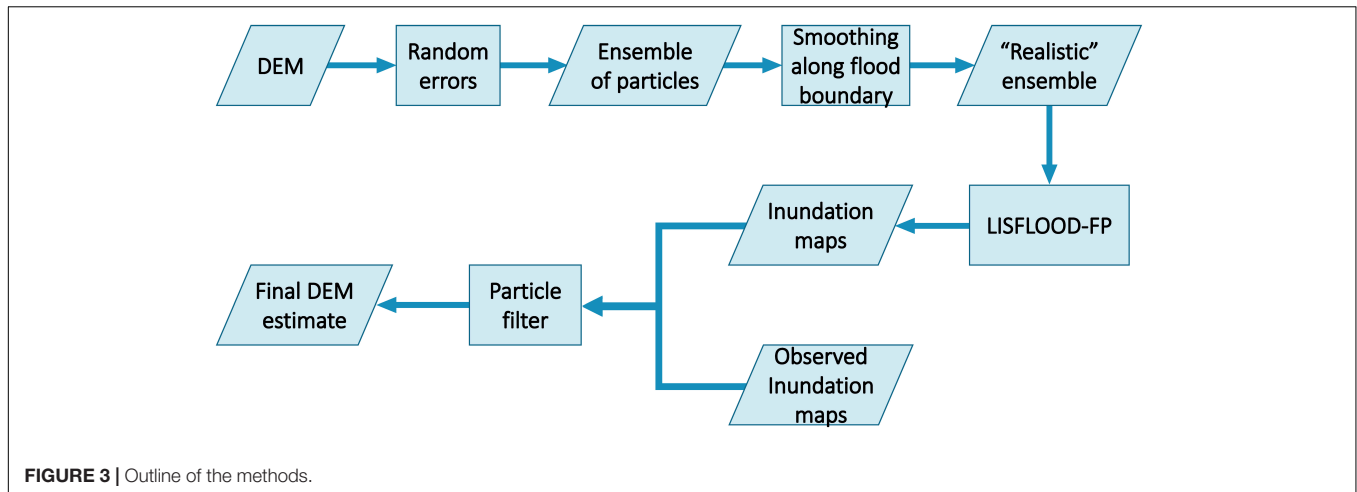


modeling. Airborne light detection and ranging (lidar) DEMs offer the best horizontal resolution and vertical accuracy. However, high resolution lidar DEMs are not available globally and are expensive to obtain. Globally, the best available DEMs are obtained from satellite data: the shuttle radar topography

mission (SRTM, spatial resolution 30 m) (Rodriguez et al., 2006) and multi-error-removed improved-terrain (MERIT, spatial resolution 90 m) (Yamazaki et al., 2017) DEM are a few examples of freely available DEMs. The global average for vertical relative error in SRTM is about 6 m (Rodriguez et al., 2006). TanDEM-X DEM produced by DLR (German Aerospace Center) has better spatial resolution (10–12 m) and vertical accuracy ( $\sim 2$  m) (Krieger et al., 2006; Eineder et al., 2012). However, it is a commercial product and is not freely available. Because the vertical inaccuracies of the SRTM DEM, flood inundation modeling using SRTM produces spatial inconsistencies (Sanders, 2007; Yamazaki et al., 2012; Yan et al., 2015; Fernández et al., 2016; Sampson et al., 2016). Hence, these DEMs are not suitable for flood simulations as they do not represent the topography well (Sanders, 2007). There have been calls to produce global scale high resolution DEMs because of its impact on emergency services and scientific research (Schumann et al., 2014).

Spaceborne remote sensing observations of inundation extent contain indirect information about floodplain topography. Remotely sensed data is widely used to study floods (Schumann and Domeneghetti, 2016) for applications such as flood risk assessment, emergency flood response, and flood mapping, but inference of floodplain topography from inundation has rarely been attempted; Mason et al. (2016) is an example of one such study. Spatiotemporal inundation patterns in floodplains are responses to a combination of factors and input variables like flow rate in the river channels, soil type, vegetation, etc.: floodplain topography determines where floodwaters flow after rivers flood their banks. For this reason, inundation patterns contain indirect information about floodplain topography. As a specific example, the boundaries of flood inundation are essentially the contours of ground elevation, if the water level is assumed to be flat (this idea can easily be extended to account for river slope, as well). Using inundation “contours” in this way is the inverse of the well-known body of the literature that uses inundation intersected with a high precision DEM to infer water levels (Matgen et al., 2007; Cohen et al., 2018). It is intuitive that these contours could be used to constrain relative variations in floodplain topography: for example, noisy elevations could be smoothed by averaging along inundation edges. Mason et al. (2016) used synthetic aperture radar (SAR) derived flood extents to improve the height accuracy in TanDEM-X DEM. They tested the method in a region where the errors had a mean and standard deviation of  $\sim 0.5$  and  $\sim 2$  m, respectively. The mean difference between TanDEM-X and lidar DEM reduced from 0.5 to 0.3 m, and their standard deviation reduced from 2 to 1.2 m. However, it is not certain the method would work for regions with higher height errors, like SRTM, which has mean and standard deviation of errors in the range of  $\sim 1.2$  and  $\sim 4$  m, respectively.

Because inundation images reflect the complex flow paths that water takes during flooding events that can only be captured by flood models, methods such as Mason et al. (2016) (referred to as “smoothing methods,” hereafter) are unlikely to extract all possible topographic information from inundation imagery. Because two-dimensional flood models encapsulate floodplain processes, it is natural to attempt to use such models to help extract topographic information from inundation. Indeed, the



objective here is to infer floodplain topography using inundation maps, while flood models do the inverse: predict inundation using floodplain topography. Thus, this is a classic example of an “inverse problem” (Yeh, 1986). Data assimilation is a technique that can be used to solve inverse problems; assimilation combines measurements and models to produce an estimate of the system which is better than just the measurement or model alone.

To our knowledge, assimilation has not been used to estimate floodplain DEMs, though related work has been done. Durand et al. (2008) assimilated water surface elevation observations along with LISFLOOD-FP hydrodynamic model to estimate channel bathymetry. Observations from SAR images of river inundation were assimilated with 2-D shallow water equations to identify optimal Manning’s coefficients (Lai and Monnier, 2009; Hostache et al., 2010; Monnier et al., 2016). One obvious impediment to using flood models to infer floodplain topography is the high dimensionality of the problem: in principle, the elevation value for each grid cell in the floodplain model must be estimated. An additional consideration is that flood models are computationally expensive, and many assimilation algorithms require either repeated model runs or ensembles of runs. A final concern is the high degree of non-linearity between the observed inundation and the floodplain topography, as some approaches [e.g., the ensemble-based assimilation of Durand et al. (2008)] are based on linear estimation theory. The non-linearity can be accounted for by using a so-called “Particle Batch Smoother” (PBS), as described in Margulis et al. (2015), which is a non-Gaussian estimator that directly approximates Bayes theorem.

In the present study, we present and test (using synthetic observations) a new algorithm designed to infer floodplain topography using globally available DEMs and inundation imagery. The algorithm consists of two steps: smoothing and data assimilation, that capitalize on the strengths of each method.

## EXPERIMENT DESIGN

We tested our algorithm for a synthetic case of small domain. This allowed us to explore the sensitivity of the algorithm to

errors of various magnitude. We used the Buscot model, a tested example model distributed with LISFLOOD-FP, as our synthetic test case. LISFLOOD-FP (Bates and De Roo, 2000; Bates et al., 2010) is a raster-based inundation model. We considered the DEM used in this model as the truth. The model had a defined river channel, and the flow in it was defined by the inflow boundary condition. The flow into the channel was defined by the inflow hydrograph with a flow of 20 m<sup>3</sup>/s at time 0, 200 m<sup>3</sup>/s at its peak and back to 20 m<sup>3</sup>/s at the end of the 5-day simulation. **Figure 1A** shows the DEM, and **Figure 1B** shows the maximum flooded extent for this test case.

To obtain best results from this method, we require multiple unique flood extent observations. We used 9 flood inundation maps obtained between day 1 and peak inundation on day 3 as observations. Our primary objective was to test the efficacy of the algorithm itself, and we did not focus on studying the impact of less or more flood inundation observations. In order to focus on the effect of prior DEM error on the analysis, we did not add white noise to the classified imagery; we leave for future work how observational uncertainty and temporal revisit would impact the algorithm accuracy. **Figure 2** shows flood inundation area for the simulation period, and the maps that were used as observations.

In the design of the synthetic experiment, we attempt to simulate a realistic situation where we attempt to correct a noisy “prior” estimate of the floodplain DEM. We accomplish this by taking the DEM distributed with the Buscot model to be the “truth.” We then create a prior estimate of the DEM by adding errors to the truth. Here we chose to add spatially uncorrelated errors when creating the prior; the level of the errors varies among the various cases. We define the “nominal case” to be addition of 0.5 m bias and 1 m standard deviation of errors, which is referred to as the prior henceforth. We performed sensitivity analysis by considering 8 additional cases, by exploring bias ranging from 0.5, 1, and 2 m, and standard deviation of 1, 2, and 4 m. The case with bias of 0.5 and 2 m is similar to the TanDEM-X errors, which was used by Mason et al. (2016). The cases with bias of 1 and 2 m, and standard deviation of 4 m is similar to SRTM.

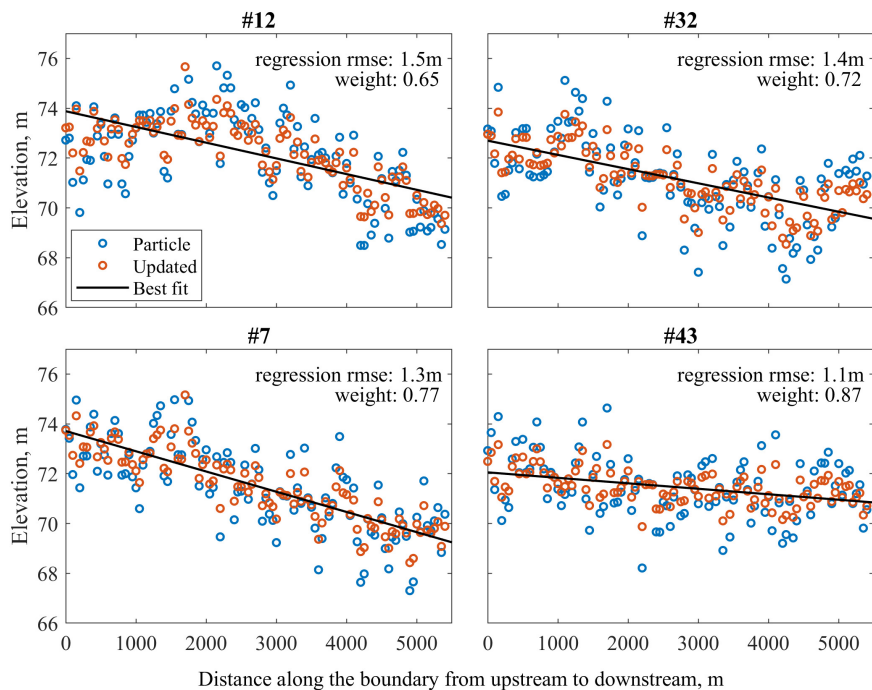


**FIGURE 4** | Elevations along the boundary for four sample ensemble members for the nominal case. Weight refers to the inverse of RMSE of the best fit line, and is used to smooth the elevations along the boundary.

We evaluated the performance of the algorithm by calculating bias, standard deviation of DEM errors and root mean squared error (RMSE) for all the pixels modified by the algorithm. We also evaluated the DEM's ability to predict inundation by using true positive rate (TPR), a statistical measure of binary classification. TPR is the proportion of predicted inundation area from the model that is accurate (from observations).

## MATERIALS AND METHODS

Our approach merges smoothing and data assimilation to better extract floodplain topography information from inundation maps. We will use the PBS concept described by Margulis et al. (2015) for a different estimation problem. The PBS is related to the Ensemble Kalman batch smoother used by Durand et al. (2008) to infer channel bathymetry from inundated area, but relies upon a fully Bayesian approach that does not assume linearity between the observations and the quantities to be estimated. The PBS represents the relationships between observations and model parameters, as well as the associated uncertainty, using a set of model simulations, which are referred to as “particles.” Each particle represents an independent random realization of the sample. The basic idea is to generate a moderately sized set of particles, where each particle is a random perturbation of the prior DEM. Here we adapt the usual PBS algorithm by first performing smoothing on each of the particles prior to the PBS estimation. Then the LISFLOOD-FP model is

run on each of the smoothed particles. Finally, the PBS estimate of the DEM is computed by comparing the LISFLOOD-FP model run output of each particle to the map of inundation observation. The PBS estimate can be thought of as a weighted average of all the DEM particles, where the weights are based upon the accuracy of LISFLOOD-FP in simulating the inundation. **Figure 3** shows an outline of the method we use to estimate an updated DEM using the PBS. One note of clarification: we use weighted averages in two contexts. In the first case, they are used for the smoothing elevations along flood boundaries, and they are referred to as weights (ensemble and regression). In the data assimilation step, we use particle weights to obtain the final estimate, and these weights are referred to as particle weights.

## Generating Particles

It has been established from empirical evidence that DEM errors are not completely random, and often have spatial correlation (Hunter and Goodchild, 1997; Fisher, 1998; Kyriakidis et al., 1999; Carlisle, 2005; Erdoğan, 2010). Hence, we added spatially correlated errors to the prior (It should be noted that, in this implementation of a synthetic case, we created the prior by adding uncorrelated random errors to the “true” DEM.), and generated an ensemble of 50 particles. We added errors with zero mean, 1 m standard deviation and 250 m correlation length to the prior. We also added a constant bias to each particle; the constant bias was randomly generated in the same range as the bias of the prior (−0.5 to 0.5 m for the nominal case).

The set of randomly perturbed DEMs thus obtained might be inefficient as the process may generate many unrealistic DEM particles. Data assimilation style approach will require a large set of particles to capture the complex spatial pattern of topography, making the process computationally inefficient. One way to deal with this problem is to make the ensemble of particles more realistic. We make this ensemble of particles more realistic by using the process described in Section “Smoothing Along Flood Boundary”.

### Smoothing Along Flood Boundary

We exploited the indirect information about elevations along the flood boundary to produce a set of realistic particles. For each particle in the ensemble, we extracted the elevations along the flood boundary. We extracted two adjacent pixels along the boundary: one flooded pixel on the edge (the “wet boundary”), and the adjacent pixel on the non-flooded side (the “dry boundary”). Then, we performed linear regression along both boundaries, considering the wet and dry boundaries separately. We consider the length along the boundary going from upstream to downstream as the independent variable and the extracted elevations as the dependent variable. We modified each particle by updating the elevations along the flood boundary as the weighted average of extracted elevations, and its regressions. By doing this, the noise in elevations along the boundary was reduced (Figure 4). The weights are expressed as the inverse of RMSE of the prior, and of the regression. We used nine flood inundation maps to perform this operation.

We used the estimate of bias and standard deviation of errors for the prior to calculate RMSE of the prior. We use this RMSE to compute the ensemble weight,  $w_{en}$ , as the inverse of RMSE of the prior. For the regressed line along the boundary, the weight is defined as:

$$w_{fit,j} = \frac{1}{rms(z_{en} - z_{fit,j})} \tag{1}$$

where  $w_{fit,j}$  is the regressed weight of  $j$ th particle,  $z_{en}$  is the elevation along flood boundary in the prior, and  $z_{fit,j}$  is the elevation along flood boundary in the  $j$ th particle. Figure 4 shows RMS of difference between regression ( $z_{fit,j}$ ) and prior ( $z_{en}$ ) elevations along the boundary, and its corresponding weight ( $w_{fit,j}$ ) for four sample particles. The updated elevation along the flood boundary,  $z_j^+$ , is calculated as:

$$z_j^+ = \frac{w_{en}z_{en,j} + w_{fit,j}z_{fit,j}}{w_{en} + w_{fit,j}} \tag{2}$$

Figure 4 shows the elevations along the boundary for the particle, regressed and updated elevations for four sample particles in the nominal case. The flood boundary of each ensemble member was replaced with this value of  $z_j^+$  from that particle to obtain an updated set of particles.

When we modify elevations along the observed flood boundary, we introduce sub-optimality into the analysis, because the errors in the smoothed DEMs are now dependent on errors in the observations. Thus the errors in the

LISFLOOD-FP predictions are also correlated with the errors in the observations, whereas the PBS assumes that they are not correlated. However, we assume that the degree of sub-optimality introduced by using the observations is relatively small compared to the large errors in the prior DEM.

### Data Assimilation

We ran a forward simulation of LISFLOOD-FP using the updated particles ( $z_j^+$ ) to obtain inundation maps for each particle. All the parameters (except the DEM) in the model were the same as in the simulation using “true” DEM. The inundation maps from this set of simulations were used along with observed inundation maps using PBS (Durand et al., 2008; Margulis et al., 2015) to estimate the updated DEM. PBS is a non-Gaussian estimator which directly approximates Bayes theorem. Initially, all ensemble members are assigned equal particle weights. We evaluate the likelihood of each particle by simulating flood inundation maps, and calculating the agreement between the modeled and observed flood inundation. True positive rate (TPR) is used to define the agreement between the modeled and observed inundation. We used exponential probability distribution to update the weights. The value of the probability density function  $w_j$  at any point  $t_j=1-TPR_j$  is defined as the particle weight of the  $j$ th particle. The probability density function for exponential distribution is defined as:

$$w_j = \lambda e^{-\lambda t_j} \text{ for } t_j > 0 \tag{3}$$

where  $t_j$  is the random variable,  $\lambda$  is a rate parameter and  $\lambda = 1/\mu = 1/\sigma$ ,  $\mu$  being the expected value of the distribution and  $\sigma$  the standard deviation. We then update the particle weight according to its likelihood of producing accurate inundation maps. The rate parameter  $\lambda$  is used to represent uncertainty in observations, and we use a value of 0.1 in the current study. Here, we calibrated the value of  $\lambda$  for the data assimilation to produce largest error correction. This means that our confidence in observations is high. The value of  $\lambda$  can be modified to represent the confidence in the observations. Higher value of  $\lambda$  produces less contrast between weights at  $t$  equal to 0 and 1. Hence, the weights are close to each other, indicating a lower confidence in observations. The updated particle weight is proportional to the likelihood of the model predicting the observation. Particles that produce inundation maps with high agreement have large particle weights; particles that have poor agreement have small particle weights. The posterior or updated DEM is the weighted average of the prior DEMs, calculated as shown in (4).

$$DEM^+ = \frac{\sum w_j DEM_j^-}{\sum w_j} \tag{4}$$

where  $DEM^+$  is the updated estimate,  $DEM_j^-$  and  $w_j$  are  $j$ th particle and its particle weight of  $j$ th particle. Figure 5 shows the agreement in flood extent between the model and observations for a sample of nine particles. TPR, and the corresponding particle weight ( $w_j$ ) assigned to that particle for those nine particles are shown in their respective panel in Figure 5. It can be

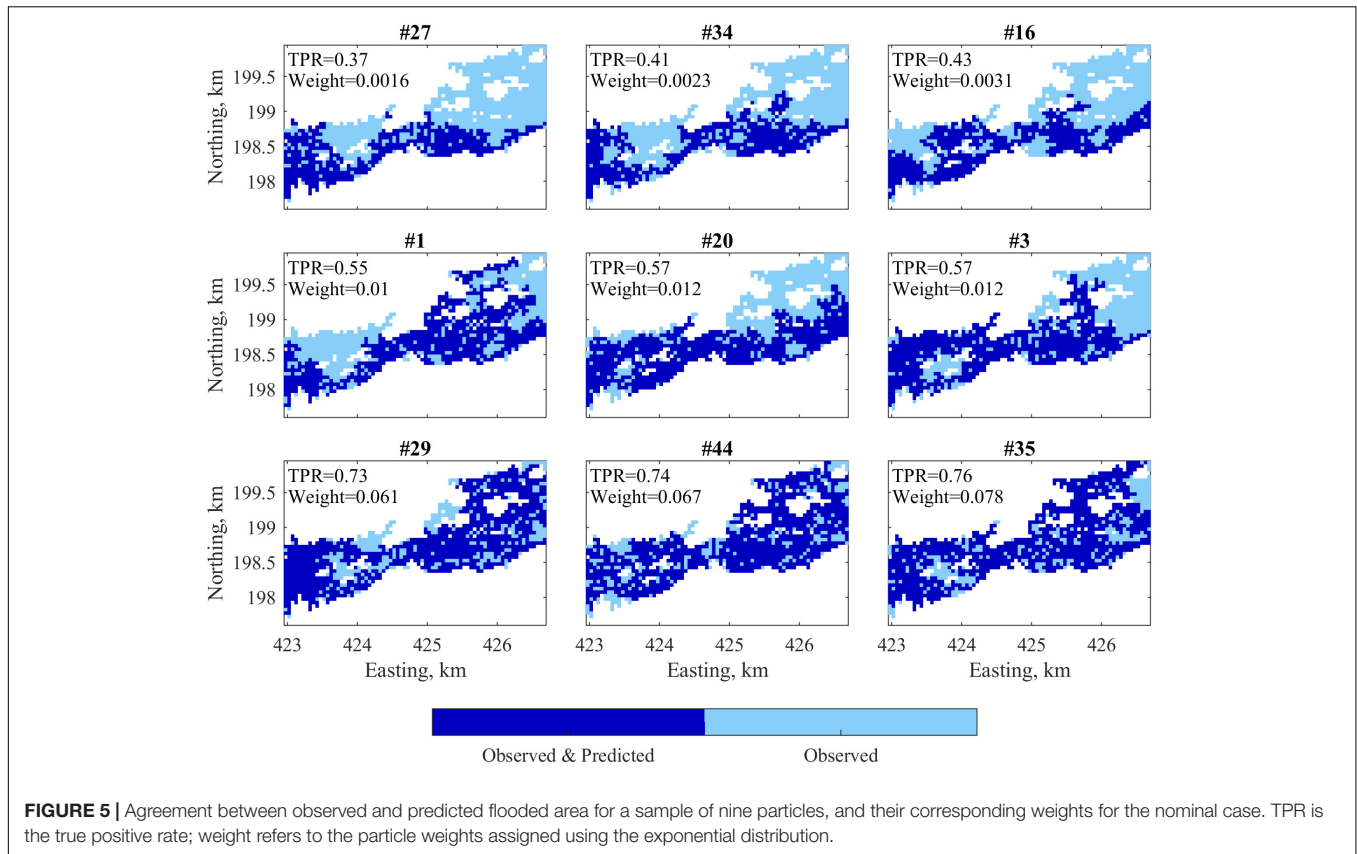


**FIGURE 5 |** Agreement between observed and predicted flooded area for a sample of nine particles, and their corresponding weights for the nominal case. TPR is the true positive rate; weight refers to the particle weights assigned using the exponential distribution.

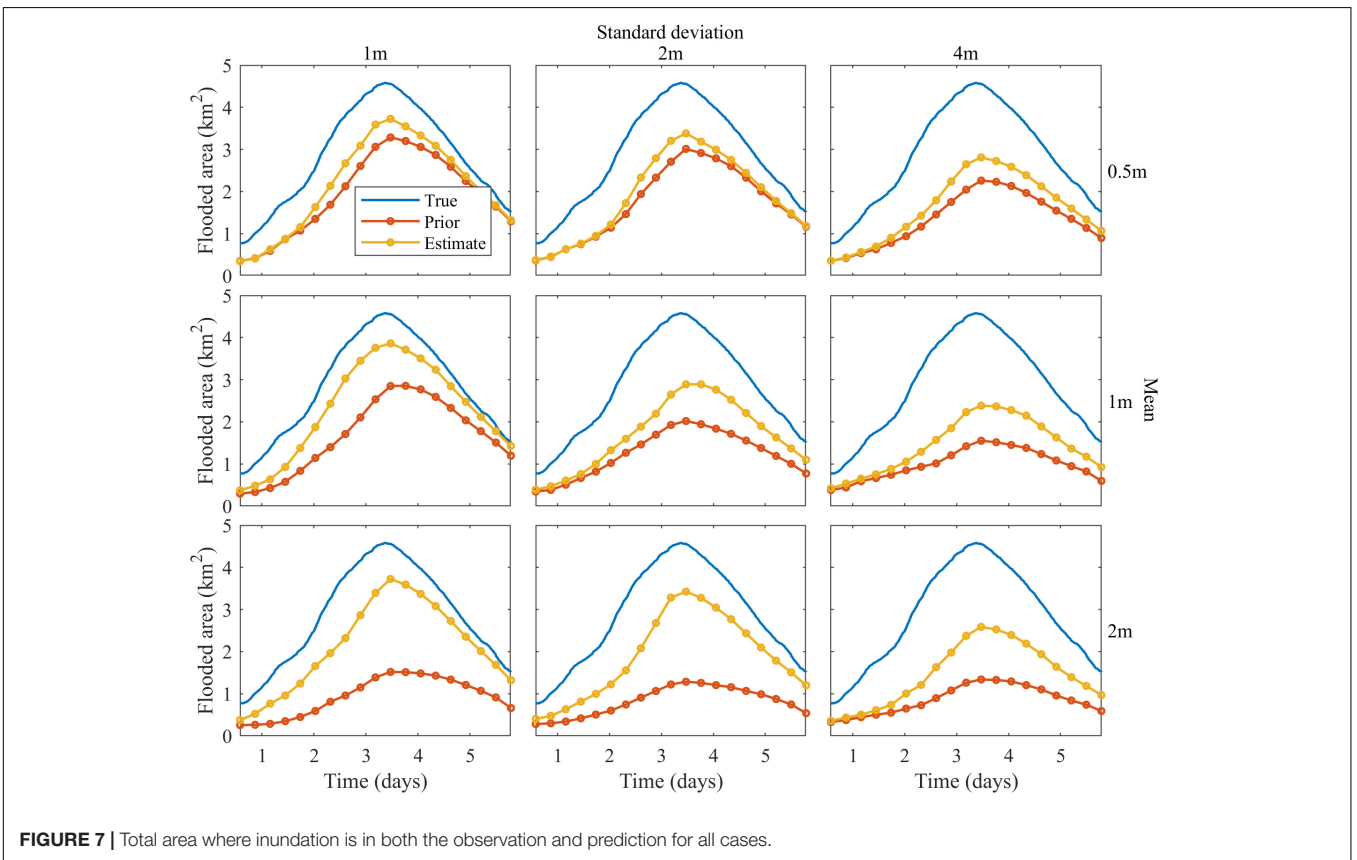
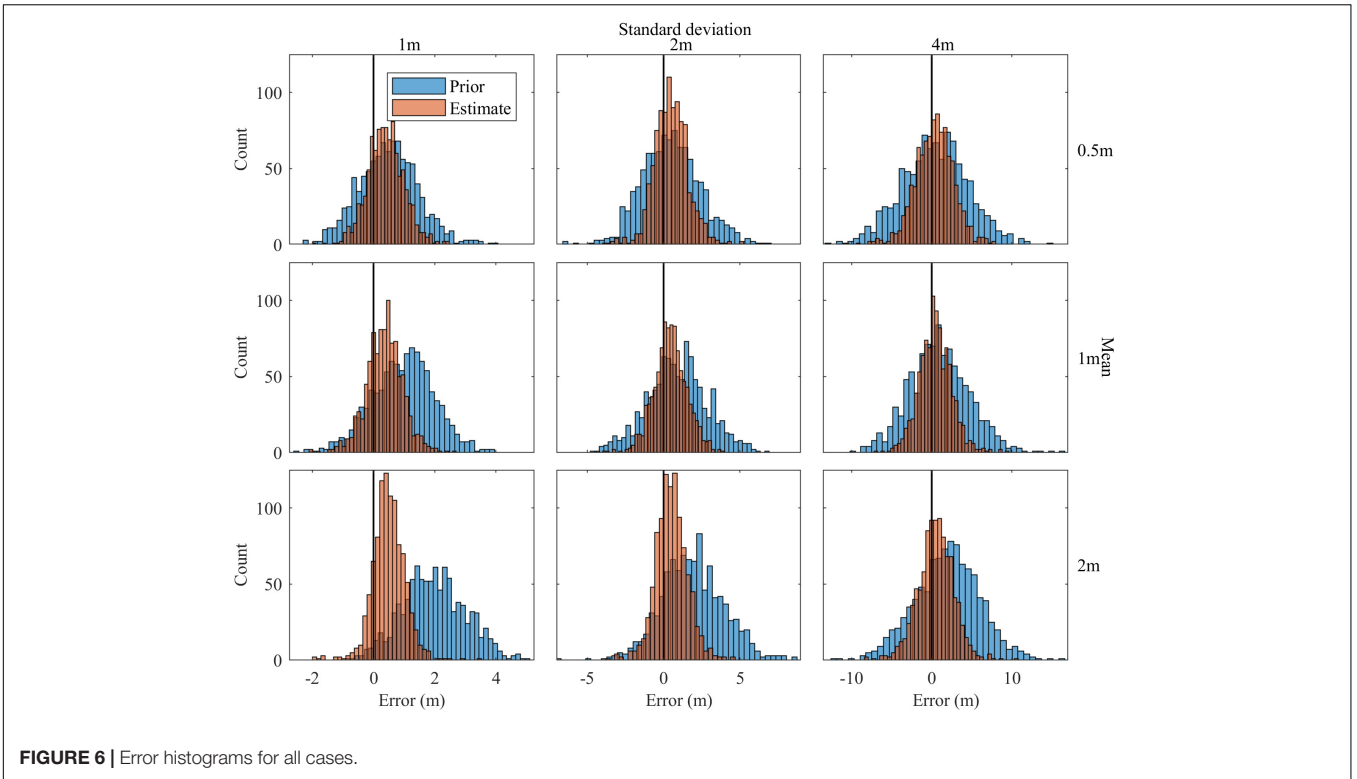
**TABLE 1 |** Statistics for height errors along the flood boundary before and after smoothing.

		Standard deviation (m)									
		1			2			4			
		Prior	Smoothed	Final estimate	Prior	Smoothed	Final estimate	Prior	Smoothed	Final estimate	
		Bias (m)									
		0.50	0.50	0.52	0.40	0.55	0.56	0.49	0.42	0.38	0.32
		1.00	0.98	0.96	0.35	0.93	0.93	0.43	0.94	0.90	0.45
		2.00	1.94	1.95	0.50	2.00	2.00	0.50	2.02	2.02	0.48
		Standard deviation (m)									
Mean (m)	0.50	0.98	0.59	0.59	1.92	1.13	1.13	4.13	2.41	2.40	
	1.00	1.03	0.59	0.60	1.96	1.09	1.09	3.76	2.04	2.04	
	2.00	1.03	0.50	0.53	2.03	1.07	1.07	4.03	2.20	2.24	
		RMSE (m)									
		0.50	1.10	0.78	0.71	1.99	1.26	1.23	4.15	2.44	2.42
		1.00	1.42	1.13	0.69	2.16	1.43	1.18	3.88	2.23	2.09
		2.00	2.20	2.01	0.73	2.84	2.27	1.18	4.51	2.99	2.29

seen that the particles that produce inundation maps with high agreement are given high particle weights, and vice versa. The final estimate DEM is obtained by using these particle weights to obtain a weighted mean of the updated ensemble of particles.

### Sensitivity Analysis

In most continents, the mean SRTM error is less than 2 m, and standard deviation is ~4 m (Rodriguez et al., 2006). To ensure that our methodology works in these ranges, we implemented



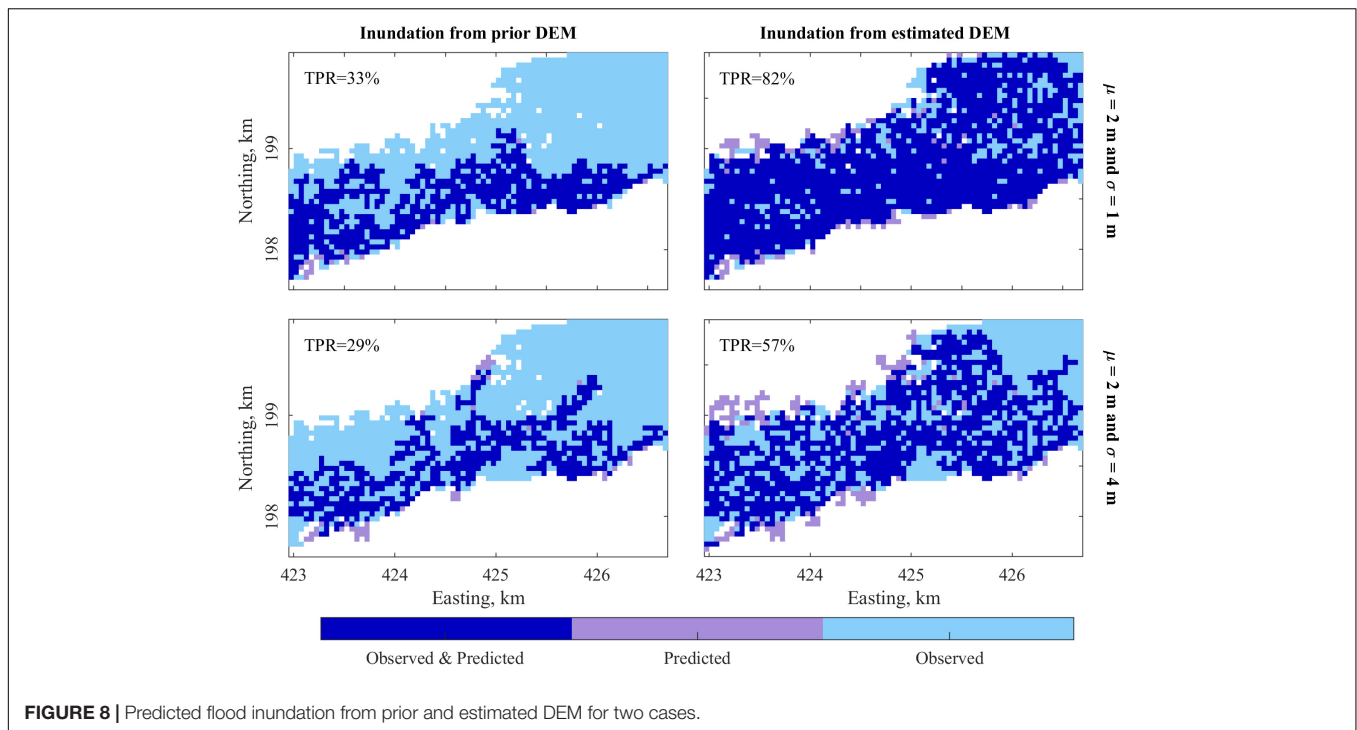


**FIGURE 8** | Predicted flood inundation from prior and estimated DEM for two cases.

the algorithm for several cases with varying levels of error mean and standard deviation in the prior. We created eight additional priors to the nominal case. The nine cases had errors of mean 0.5, 1, and 2 m, and standard deviation of 1, 2, and 4 m added to the “true” DEM. We applied the algorithm described in Section “Generating Particles, Smoothing Along Flood Boundary, and Data Assimilation” to the eight additional priors to obtain the final estimate DEM for those respective cases.

## RESULTS AND DISCUSSION

Root mean squared error for the prior for the nominal case (errors of 0.5 m mean and 1 m standard deviation) was 1.10 m. The set of particles generated from this prior had an RMSE of was 1.10 m. The RMSE of height errors along the flood boundaries reduced to 0.78 m in the updated set of particles where we smoothed elevations along the flood boundary. **Table 1** shows height errors in the initial ensemble and updated ensemble of particles. After putting this modified set of particles through the PBS, the RMSE further reduced to 0.71 m. The bias reduced from 0.5 to 0.4 m and standard deviation of errors went down from 0.98 to 0.59 m.

Sensitivity analysis also showed similar trends, improving upon priors in terms of bias, standard deviation of errors and RMSE. We found that the process of smoothing did not have an effect on the bias before and after smoothing. The difference between prior bias and smoothed bias is less than 4 cm for all the cases (**Table 1**). However, the standard deviation of errors went down after smoothing. The standard deviation of error was reduced by 40 to 49% in all the cases (**Table 1**). Generally, as the standard deviation in the prior increased, the amount

of reduction increased. The amount of reduction also increased as the bias in the prior increased. **Table 1** shows the values of standard deviation for all the tested cases for the prior and smoothed ensembles.

When this smoothed set of particles was put through a PBS, the bias reduced in the final estimate from the prior and the smoothed ensemble. **Table 1** shows the details about error for the final estimate of elevations along the flood boundary. In general, the relative reduction in bias increased as the prior’s bias increased. For the cases with 0.5 m bias, reduction in bias for the final estimate ranged between 11 and 24%. In all other cases (1 and 2 m bias), the bias reduced to 0.5 m or less. The reduction in bias ranged between 52 and 76%. However, there was no effect of the PBS on the standard deviation of error. The reduction is standard deviation of errors was less than 4 cm for all the cases (**Table 1**).

**Figure 6** shows the histograms for errors in all tested cases. It is clear from **Figure 6** that there is a reduction in bias and standard deviation of errors from the prior to the final estimate. A greater number of cells have lower errors, and the number of cells with

**TABLE 2** | True positive rate (TPR) at peak inundation.

		Standard Deviation (m)					
		1		2		4	
		Prior	Estimate	Prior	Estimate	Prior	Estimate
Mean (m)	0.5	72	82	66	74	50	62
	1	63	85	44	63	34	52
	2	33	82	28	75	29	57



high errors are reduced. The algorithm improved upon the prior in all the cases, and the reduction in RMSE varied from 35 to 67%.

When we used the final estimate DEMs to predict flood inundation, there was a consistent increase in TPR when compared to the prior. **Figure 7** shows the predicted inundation area for the simulation period. In all the cases, the correctly predicted flood inundation area (i.e., the total area where inundation is in observation and prediction) was greater for the final estimate than the prior. **Figure 8** shows the flood inundation maps obtained from the prior and final estimated DEMs for two cases. The top row shows the peak inundation maps for the case with error of 2 m mean and 1 m standard deviation on 2.3 days. The TPR goes up from 33 to 82%. The second row corresponds to the case with error of mean 2 m and standard deviation 4 m, the case we believe is similar to SRTM DEM. In this case, the TPR increases from 29 to 57%. **Table 2** shows the change in TPR for peak inundation in all the cases. There was greater improvement of TPR with increase in bias of the priors. TPR for the peak inundation obtained from the final estimate DEM for all the cases with 1 m error standard deviation was greater than 82%. For the cases with 2 m error standard deviation, TPR for the peak inundation obtained from the final estimate DEM was between 63 and 75%; for cases with 4 m standard deviation of errors, it ranged between 52 and 62% (**Table 2**). It can be seen that there is a significant increase in TPR from prior to final estimate in all cases.

## CONCLUSION

We successfully implemented a new algorithm to improve topography information in a floodplain by exploiting indirect information of ground elevations from observed flood extents. In synthetic tests, the algorithm reduced the bias, standard deviation of errors and RMSE. Our primary motivation to produce better topography was to obtain DEMs that are more suitable for flood inundation simulations. The improved DEM we obtained from this algorithm also predicted flood inundation much better than

## REFERENCES

- Bates, P. D., and De Roo, A. P. J. (2000). A simple raster-based model for flood inundation simulation. *J. Hydrol.* 236, 54–77. doi: 10.1016/S0022-1694(00)00278-X
- Bates, P. D., Horritt, M. S., and Fewtrell, T. J. (2010). A simple inertial formulation of the shallow water equations for efficient two-dimensional flood inundation modelling. *J. Hydrol.* 387, 33–45. doi: 10.1016/j.jhydrol.2010.03.027
- Carlisle, B. H. (2005). Modelling the spatial distribution of DEM error. *Trans. GIS* 9, 521–540. doi: 10.1111/j.1467-9671.2005.00233.x
- Cohen, S., Brakenridge, G. R., Kettner, A., Bates, B., Nelson, J., McDonald, R., et al. (2018). Estimating floodwater depths from flood inundation maps and topography. *J. Am. Water Resour. Assoc.* 54, 847–858. doi: 10.1111/1752-1688.12609
- Durand, M., Andreadis, K. M., Alsdorf, D. E., Lettenmaier, D. P., Moller, D., and Wilson, M. (2008). Estimation of bathymetric depth and slope from data assimilation of swath altimetry into a hydrodynamic model. *Geophys. Res. Lett.* 35:L20401. doi: 10.1029/2008GL034150
- Eineder, M., Fritz, T., Abdel Jaber, W., Rossi, C., and Breit, H. (2012). “Decadal Earth topography dynamics measured with TanDEM-X and SRTM,” in

the prior. We implemented the algorithm for nine different cases with varying mean and standard deviation of errors, and obtained similar trends in the reduction of bias and standard deviation of errors. In fact, the magnitude and percentage reduction in bias increases in cases with higher errors. The results from the synthetic tests show potential, and we believe that the method could be used to improve DEM accuracy. For example, SRTM DEM could be used as prior, along with flood inundation observations obtained from Landsat or radar to obtain a DEM with better elevation accuracy.

Digital elevation models are the primary source of topographic information, and accurate DEMs are hard to obtain in the developing world. Globally available open-source products are easy to obtain, but are not accurate. Hence, they are not suitable for flood inundation modeling (Fernández et al., 2016). It is not always physically or financially feasible to obtain lidar DEMs in data-poor regions. An algorithm to improve already available DEMs is one way we can study these regions, and make better predictions. This study has produced promising results, and we believe this algorithm can be applied to real world cases to improve floodplain topography. This will provide us with higher accuracy DEMs in data-poor floodplains which are suitable for flood inundation simulations.

## AUTHOR CONTRIBUTIONS

All authors designed the model and the computational framework and wrote the manuscript. AS performed the analysis and interpretation of data.

## FUNDING

This work was funded by NASA Headquarters under the NASA Earth and Space Science Fellowship Program (Grant 80NSSC17K0322).

- International Geoscience and Remote Sensing Symposium (IGARSS)*, (Munich), doi: 10.1109/IGARSS.2012.6351130
- Erdoğan, S. (2010). Modelling the spatial distribution of DEM error with geographically weighted regression: an experimental study. *Comput. Geosci.* 36, 34–43. doi: 10.1016/j.cageo.2009.06.005
- Fernández, A., Najafi, M. R., Durand, M., Mark, B. G., Moritz, M., Jung, H. C., et al. (2016). Testing the skill of numerical hydraulic modeling to simulate spatiotemporal flooding patterns in the Logone floodplain, Cameroon. *J. Hydrol.* 539, 265–280. doi: 10.1016/j.jhydrol.2016.05.026
- Fisher, P. (1998). Improved modeling of elevation error with geostatistics. *Geoinformatica* 2, 215–233. doi: 10.1023/A:1009717704255
- Hostache, R., Lai, X., Monnier, J., and Puech, C. (2010). Assimilation of spatially distributed water levels into a shallow-water flood model. Part II: use of a remote sensing image of mosel river. *J. Hydrol.* 390, 257–268. doi: 10.1016/j.jhydrol.2010.07.003
- Hunter, G. J., and Goodchild, M. F. (1997). Modeling the uncertainty of slope and aspect estimates derived from spatial databases. *Geogr. Anal.* 29, 35–49. doi: 10.1111/j.1538-4632.1997.tb00944.x
- Krieger, G., Moreira, A., Fiedler, H., Hajnsek, I., Zink, M., and Werner, M. (2006). “TanDEM-X: Mission concept, product definition and performance prediction,”

- in *Proceedings European Conference on Synthetic Aperture Radar (EUSAR)*, (Dresden).
- Kyriakidis, P. C., Shortridge, A. M., and Goodchild, M. F. (1999). Geostatistics for conflation and accuracy assessment of digital elevation models. *Int. J. Geogr. Inf. Sci.* 13, 677–707. doi: 10.1080/136588199241067
- Lai, X., and Monnier, J. (2009). Assimilation of spatially distributed water levels into a shallow-water flood model. Part I: mathematical method and test case. *J. Hydrol.* 377, 1–11. doi: 10.1016/j.jhydrol.2009.07.058
- Margulis, S. A., Giroto, M., Cortés, G., and Durand, M. (2015). A particle batch smoother approach to snow water equivalent estimation. *J. Hydrometeorol.* 16, 1752–1772. doi: 10.1175/JHM-D-14-0177.1
- Mason, D. C., Trigg, M., Garcia-Pintado, J., Cloke, H. L., Neal, J. C., and Bates, P. D. (2016). Improving the TanDEM-X digital elevation model for flood modelling using flood extents from synthetic aperture radar images. *Remote Sens. Environ.* 173, 15–28. doi: 10.1016/j.rse.2015.11.018
- Matgen, P., Schumann, G., Henry, J. B., Hoffmann, L., and Pfister, L. (2007). Integration of SAR-derived river inundation areas, high-precision topographic data and a river flow model toward near real-time flood management. *Int. J. Appl. Earth Obs. Geoinf.* 9, 247–263. doi: 10.1016/j.jag.2006.03.003
- Monnier, J., Couderc, F., Dartus, D., Larnier, K., Madec, R., and Vila, J. P. (2016). Inverse algorithms for 2D shallow water equations in presence of wet dry fronts: application to flood plain dynamics. *Adv. Water Resour.* 97, 11–24. doi: 10.1016/j.advwatres.2016.07.005
- Rodriguez, E., Morris, C., and Belz, J. (2006). An assessment of the SRTM topographic products. *Photogramm. Eng. Remote Sensing* 72, 249–260.
- Sampson, C. C., Smith, A. M., Bates, P. D., Neal, J. C., and Trigg, M. A. (2016). Perspectives on open access high resolution digital elevation models to produce global flood hazard layers. *Front. Earth Sci.* 3:85. doi: 10.3389/feart.2015.00085
- Sanders, B. F. (2007). Evaluation of on-line DEMs for flood inundation modeling. *Adv. Water Resour.* 30, 1831–1843. doi: 10.1016/j.advwatres.2007.02.005
- Schumann, G. J. P., Bates, P. D., Neal, J. C., and Andreadis, K. M. (2014). Technology: fight floods on a global scale. *Nature* 507:169. doi: 10.1038/507169e
- Schumann, G. J.-P., and Domeneghetti, A. (2016). Exploiting the proliferation of current and future satellite observations of rivers. *Hydrol. Process.* 30, 2891–2896. doi: 10.1002/hyp.10825
- Yamazaki, D., Baugh, C. A., Bates, P. D., Kanae, S., Alsdorf, D. E., and Oki, T. (2012). Adjustment of a spaceborne DEM for use in floodplain hydrodynamic modeling. *J. Hydrol.* 436–437, 81–91. doi: 10.1016/j.jhydrol.2012.02.045
- Yamazaki, D., Ikeshima, D., Tawatari, R., Yamaguchi, T., O’Loughlin, F., Neal, J. C., et al. (2017). A high-accuracy map of global terrain elevations. *Geophys. Res. Lett.* 44, 5844–5853. doi: 10.1002/2017GL072874
- Yan, K., Di Baldassarre, G., Solomatine, D. P., and Schumann, G. J. P. (2015). A review of low-cost space-borne data for flood modelling: topography, flood extent and water level. *Hydrol. Process.* 29, 3368–3387. doi: 10.1002/hyp.10449
- Yeh, W. W.-G. (1986). Review of parameter identification procedures in groundwater hydrology: The inverse problem. *Water Resour. Res.* 22, 95–108. doi: 10.1029/WR022i002p00095

**Conflict of Interest Statement:** The authors declare that the research was conducted in the absence of any commercial or financial relationships that could be construed as a potential conflict of interest.

The handling Editor declared a past co-authorship with one of the authors MD.

Copyright © 2019 Shastri and Durand. This is an open-access article distributed under the terms of the Creative Commons Attribution License (CC BY). The use, distribution or reproduction in other forums is permitted, provided the original author(s) and the copyright owner(s) are credited and that the original publication in this journal is cited, in accordance with accepted academic practice. No use, distribution or reproduction is permitted which does not comply with these terms.